Solar Drivers of Interplanetary and Terrestrial Disturbances
ASP Conference Series, Volume 95, 1996
K. S. Balasubramaniam, Stephen L. Keil, and Raymond N. Smartt (eds.)

Calculating Solar Wind Parameters from Solar Magnetic Field Data

V. N. Obridko, A. F. Kharshiladze and D. B. Shelting.
IZMIRAN, 142092, Troitsk, Moscow Region, Russia

Abstract. It is shown that the expansion factor of the solar magnetic field is insufficient to calculate the solar wind velocity. Moreover, the magnetic field structure cannot unambiguously determine the solar wind velocity field in terms of the source surface concept and the potential magnetic field approximation in the corona. It is shown that characteristics relating the solar and near–Earth interplanetary magnetic fields undergo cyclic variations.

1. Introduction

The origin of time variations of the daily mean solar wind velocity is still unknown. The classical theory of Parker (1958) gives a single universal velocity value at the Earth orbit, that is determined by the temperature in the solar corona. On the other hand, observations show the real velocity to range from 350 to 1100 km s^{-1}. These variations are partly due to solar flares and transients. However, even if these non–stationary events are ignored, the variations are still significant (350–850 km s^{-1}).

Slow variations of the solar wind (SW) velocity can be naturally associated with the magnetic field structure elements in the Sun, in particular, with active regions, coronal holes, large–scale field boundaries, etc. A comparison made by different authors has shown that the velocity is generally higher when the solar wind originates at open magnetic field configurations (Obridko & Shelting 1987; 1988). The same qualitative conclusion follows from the theory (for review see Priest 1985). However these works do not allow a quantitative method to be developed for routine calculation of the daily mean SW velocity.

Wang & Sheeley (1990) introduced a new parameter — the solar magnetic field expansion at the Earth projection point, and revealed negative correlation between this parameter and the daily mean SW velocity for 1967–1988. This result was theoretically interpreted by Wang & Sheeley (1991). The method was used in (Wang et al. 1990) to calculate the latitude distribution of SW velocity averaged in longitude.

It should be noted, however, that Wang & Sheeley (1990) gave only a general comparison of synoptic charts of the observed and the calculated velocities. Since the measured and the calculated values display similar dependence on the solar cycle, the agreement is seemingly very good (see Fig. 2 in Wang & Sheeley 1990). However when quantitatively compared, the measured velocities averaged over 3–month intervals show poor correlation (0.57) with the values calculated from

the expansion factor. No comparison of the daily means was performed by Wang & Sheeley (1990).

In this paper, we have applied a similar procedure to compare year by year the daily means of the measured and calculated velocities for 1978–1983. The correlation coefficient between them proved not to exceed 0.4. Moreover, it seems at all doubtful that solar wind velocity variations be mainly determined by the field structure in the Sun.

2. Comparison of the Daily Mean Solar Wind Velocity and the Magnetic Field Expansion Factor

The expansion factor is determined in the form

$$f_s(\theta_s, \varphi_s) = \frac{R_\odot^2 B_r(R_\odot, \theta_\odot, \varphi_\odot)}{R_s^2 B_r(R_s, \theta_s, \varphi_s)}. \tag{0.1}$$

Here, $(q_\odot, \varphi_\odot)$ are the photospheric coordinates of the field line that passes through the (θ_s, φ_s) point at the source surface, corresponding to the Earth projection along the field; R_s is the source surface radius; and $R_\odot$ is the radius of the Sun. In our case, $R_s = 2.5R_\odot$.

The coordinates $(\theta_\odot, \varphi_\odot)$ are derived from (θ_s, φ_s) by integrating the field line equation

$$\frac{\partial r}{B_r} = \frac{r\partial\theta}{B_\theta} = \frac{r\sin\theta\partial\varphi}{B_\varphi}. \tag{0.2}$$

The values of B_r, $B_\odot$, and B_φ along the field line are calculated from the Hoeksema and Sherrer coefficients obtained under potential approximation.

The solar wind velocities, V_w, obtained by Wang & Sheeley (1990) from the expansion factor, f_s, are:

$$\begin{array}{llll} & V_w > 650\text{km/s} & & f_s < 3.5 \\ 650\text{km/s} \geq & V_w > 550\text{km/s} & 3.5 \leq & f_s < 9.0 \\ 550\text{km/s} \geq & V_w > 450\text{km/s} & 9.0/le & f_s < 10 \\ 450\text{km/s} \geq & V_w & 18 \leq & f_s \end{array} \tag{0.3}$$

To give the continuous series of V_m values, this relation must be approximated as follows:

$$V_m = 380(1 + exp(-0.093 f_s)) \tag{0.4}$$

The result of (4) agrees fairly well with the original tabulated data.

The comparison with the measured velocity, V, was made taking into account the transport time that, unlike Wang & Sheeley (1990), was found by dividing the Sun–Earth distance by the measured velocity. Note that Wang & Sheeley (1990) considered the transport time constant, equal to 5 days. Our calculations carried out with the transport time both constant, and changing as a function of the actual measured velocity, have shown that correlation coefficient depends little on the transport time hypothesis with an accuracy to the 2nd decimal place.

The highest correlation between the calculated, V_m, and the measured, V, velocities is observed at the descending branch of cycle 21 (1982–1983) and is 0.375, the total number of days being 721.

However the correlation coefficient in itself is not very much representative. In fact, the days of low–speed solar wind are much more frequent than the days of high–speed solar wind. It is necessary that the latter situations be as reliably identified as the former. For this purpose, we have developed a matrix presented in Table 1. The Table gives 3 versions of the matrix:

1a) The number of days when the observed (columns i) and the calculated (rows j) velocities fall within the given range in accordance with (3). This matrix is called n_{ij}.

1b) The percentage ratio of the number of days in a given cell to the total number of records (721).

1c) The ratio of the number of days in a given cell to the total number of days when velocity was observed in the given interval ("percentage over the column").

In the ideal case of completely reliable identification, one would obviously observe concentration to the main diagonal in the matrices, and the sum of numbers in case 1b must considerably exceed 50%. As seen from Table 1, in spite of some concentration effect observed, the sum of numbers along the main diagonal in table 1b is as small as 42.3%.

Another requirement is that all numbers along the main diagonal 1c were larger than 50%, thus, accounting for the difference in the occurrence of high and low velocities. Unfortunately, this requirement is not satisfied either. Only in the range of very low velocities, the reliability of identification is 53%.

Table 1. Relation between the measured velocities and those calculated by the Wang & Sheeley method (1990)

a)			>650.	650.-550.	550.-450.	<450.0
	>	650.	6	5	12	6
650.	–	550.	14	50	78	41
550.	–	450.	9	43	89	96
	<	450	3	29	79	161
b)			>650.	650.-550.	550.-450.	<450.0
	>	650.	.8	.7	1.7	.8
650.	–	550.	1.9	6.9	10.8	5.7
550.	–	450.	1.2	6.0	12.3	13.3
	<	450.	.4	4.0	11.0	22.3
c)			>650.	650.-550.	550.-450.	<450.0
	>	650.	18.8	3.9	4.7	2.0
650.	–	550.	43.8	39.4	30.2	13.5
550.	–	450.	28.1	33.9	34.5	31.6
	<	450.	9.4	22.8	30.6	53.0

3. The Use of Two–Dimensional Diagrams

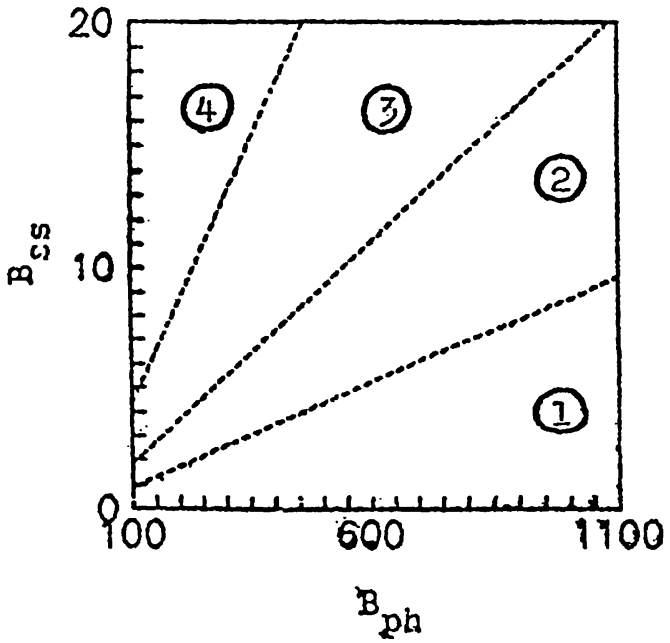

Figure 1. Velocity distribution diagram following the criterion of Wang and Sheeley (see eq.(3)). Region 1 corresponds to $f_s \geq 18$ ($V \leq 450$ km/s); region 2 — to $9 \leq f_s < 18$ (450–550 km/s); region 3 — to $3.5 \leq f_s < 9$ (550–650 km/s); and region 4 — to $f_s < 3.5$ (>650 km/s).

Thus, the situation when the velocity arises in a given range in the Sun cannot be reliably identified, proceeding from the magnetic field expansion, f_s. The expansion factor is probably the wrong parameter to choose, because the initial energy flux from the photosphere is assumed to be the same everywhere (Wang & Sheeley 1991). In fact, there are additional heating sources in active regions, i.e. in the regions of strong photospheric fields. In this case, the dependence on magnetic fields, $B_r(R_\odot, \theta_\odot, \varphi_\odot) \equiv B_{ph}$ and $B_r(B_s, \theta_s, \varphi_s) \equiv B_{ss}$, is much more complicated.

The question arises whether the solar wind velocity can at all be unambiguously determined by two parameters, B_{ph} and B_{ss}. To answer this question, let us plot two–dimensional diagrams and mark on them the recorded velocities in that or another range depending on B_{ph} and B_{ss}. The points on the diagrams, arranged in whatever complicated way, will form isolated clusters. Then, in the case of unambiguous relation of B_{ph} and B_{ss} to the solar wind velocity, these clusters should not overlap. Fig. 1 shows a diagram to illustrate the Wang–Sheeley condition (see eq. (3)). Cluster 1 in Fig. 1 corresponds to $f_s \geq 18$, i.e. to the velocities of $\leq$450 km/s; cluster 2 corresponds to $9 \leq f_s < 18$, i.e. to the velocities of 450–550 km/s; cluster 3 corresponds to $3.5 \leq f_s < 9$ (550–650 km/s); and cluster 4 to $f_s < 3.5$ (>650 km/s). The field intensity in Fig. 1 and further is given in μT.

The characteristic feature of the diagram based on (3) is that all separation lines are the rays that emanate from the reference frame origin.

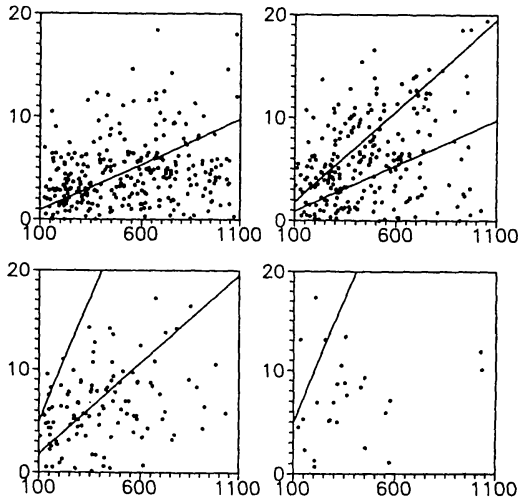

Figure 2. Distribution of measured solar wind velocities: (a) $V \leq 450$ km/s, (b) $450 < V \leq 550$ km/s, (c) $550 < V \leq 650$ km/s, and (d) $V > 650$ km/s.

In Fig. 2a, the situations corresponding to the measured velocities $V \leq 450$ km/s are illustrated and a straight line $B_{ss} = (R_\odot^2/18 \cdot R_s^2) \cdot B_{ph}$ is drawn. According to the Wang–Sheeley criterion, all points must be situated below this line. Fig. 2b represents the points of $450 < V \leq 550$ km/s and the straight lines corresponding to $f_s = 18$ and $f_s = 9$. All points must obviously appear between the two lines. Figs. 2c and 2d illustrate the points of $550 < V \leq 650$ km/s and $V > 650$ km/c, respectively, as well as the straight lines for $f_s = 9$ and $f_s = 3.5$.

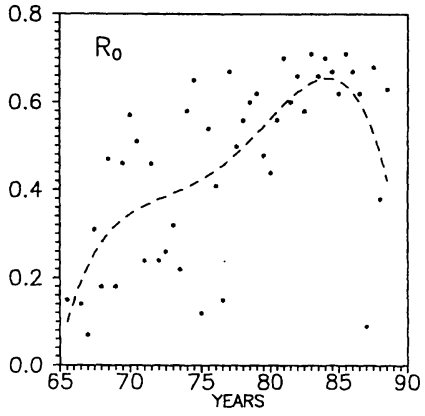

Figure 3. Correlation coefficient of the source surface field B_{ss}/r^2 and the magnetic field B_x component at the Earth orbit as a function of time.

As seen from Fig. 2, the points spread beyond the Wang–Sheeley lines, which is another evidence of invalidity of criterion (3). A more general result is inferred from Fig. 2: the solar wind velocity cannot be unambiguously de-

termined by two parameters (the field intensities in the photosphere and at the source surface), because the clusters of points in the four diagrams overlap. No cases of isolated clusters corresponding to a given SW velocity range are revealed in the (B_{ph}, B_{ss}) diagram.

4. Estimation of the Local Field Effect

We have used in our analysis the harmonic expansion coefficients of the magnetic field tabulated by Hoeksema & Sherrer (1986). These coefficients were calculated from the longitudinal magnetic field synoptic charts obtained at the John Wilcox Observatory, Stanford University. The calculations were performed in potential approximation under the assumption of a source surface existing at 2.5 $R_\odot$. This procedure allows the magnetic field to be calculated at any point of the spherical layer between the photosphere and the source surface. After the Earth projection point at the source surface is identified and the magnetic field at this point is calculated, integration of the field line equation yields the corresponding point in the photosphere, the field components along the force line being determined by the harmonic coefficients. The last step is to determine the radial magnetic field in the photosphere at the base of the field line intersecting the Earth projection. This is the field value involved in the expansion factor estimates.

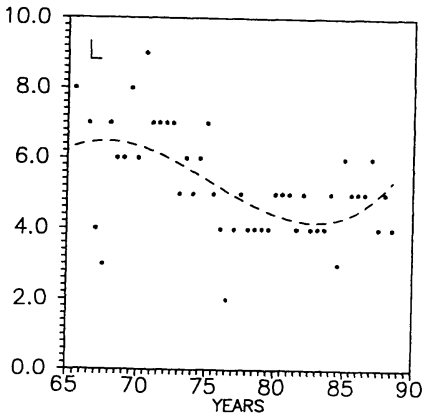

Figure 4. Shift of the correlation coefficient of the source surface field and the magnetic field B_x component at the Earth orbit as a function of time.

When put in practice, this simple and clear calculation scheme encounters certain difficulties. All calculations are performed taking into account only 10 harmonics ($l \leq 9$, $m \leq 9$). They are certainly enough for summation to give the source surface fields, however this is not the case when the photospheric fields are concerned. While comparing the calculated and the observed longitudinal magnetic fields in the photosphere, one can readily see that the former are underestimated, which implies that the first 10 harmonics are insufficient to calculate the magnetic field by using the spherical expansion method. Beginning with 300 μT, the calculated values are seen to be systematically lower than observations.

Calculated fields stronger than 900 μT are absent at all. This implies that local fields corresponding the the higher–order harmonics are systematically underestimated. Such a method, obviously, fails to provide correct expansion factor, at least during relatively high solar activity.

The contribution of local fields can be estimated by using (even if not quite reasonably) the following procedure. We were unable to trace the field line experimentally. Therefore, we substituted the measured longitudinal field, $B_\rho(R_\odot, \theta_\odot, \varphi_\odot)$, for the calculated radial field $B_r(R_\odot, \theta_\odot, \varphi_\odot)$ in (1), and then in (4). In this case, the base of the field line was not quite correctly identified, and the expansion factor was calculated with an error. Instead, we hoped to be able to estimate the contribution of local fields. However it turned out that correlation of the calculated and measured velocities did not improve by substituting the observed longitudinal for the calculated radial field.

The conclusion that SW velocities cannot be unambiguously determined by the B_{ss} and B_{ph} fields is extremely important, because these are the two basic parameters that characterize solar activity. All assumptions made in the analysis are listed below.

1) The original magnetic field data, used to calculate the expansion coefficients, were obtained at a spatial resolution of $3'$. The velocity field fine structure under discussion can be due to small–scale features in the photospheric fields.

2) The synoptic charts used in the analysis result from a synthesis of non-simultaneous observations.

3) In our analysis, we make use of longitudinal magnetic fields observations in the photosphere. All other photospheric and coronal features are calculated in potential approximation.

4) The whole calculation procedure is based on the source surface concept. However alternative models are available, and they also should be involved in the analysis (Veselovsky 1989).

5) There is a probability that the velocity field fine structure arises beyond the corona, at a distance of several solar radii. Some evidence is given in (Lotova et al. 1985; Lotova 1988).

5. Cyclic Variations in Solar Wind/Global Magnetic Field Coupling

Having direct or indirect data on photospheric magnetic fields for a long time interval, we can analyze cyclic variations in the coupling of the stationary solar wind with the calculated magnetic field on the source surface. The simplest theoretical consideration is as follows. The field beyond the source surface is mechanically transported by the solar wind and diminishes proportionally with the square distance from the Sun. Therefore, the field structure observed in the Earth neighbourhood must be totally determined by the source surface field, i.e. $B_x \approx B_y, B_z \approx 0$, and the proportionality coefficient for B_x and the source surface field, B_{ss}, must be close to $(R_{ss}/R_E)^2$, where R_E is the average Sun–Earth distance. Thus, the field at the Earth orbit can be derived from the source surface field by simple multiplication by the scale factor $\sim 1.37 \cdot 10^{-4}$. Of course, the solar wind transport time from the Sun to the Earth must be taken into account. It is either *a priori* assumed equal to 4 or 5 days, or it is calculated by dividing the Sun–Earth distance by the solar wind velocity measured at the

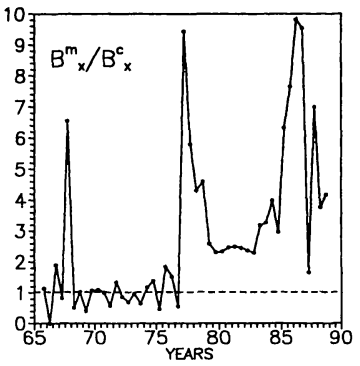

Figure 5. Ratio of the measured and the calculated magnetic field B_x components in the solar wind at the Earth orbit as a function of time.

Earth orbit on a particular day.

This simple scheme was checked only qualitatively. It was shown that, the transport time being properly selected, 70–80% of the daily mean B_x values coincided in sign with B_{ss} (e.g., see Hoeksema & Scherrer 1986). No systematic quantitative comparison of the values calculated following the mentioned scheme and the direct measurements was made over a long time interval.

We have carried out such a comparison over a time interval of 1965–1988. The main difficulty in studying cyclic variations of global magnetic fields and the heliosphere is due to the absence of sufficiently long data series. We have at our disposal synoptic maps of photospheric magnetic fields for the time interval from Aug. 1959 to Dec. 1978 (Carrington rotations 1417–1648) obtained by the group of Robert Howard at the Mount–Wilson Observatory (MWO). Another series of observations for Jan. 1975 — July 1984 (Carrington rotations 1622–1751) was performed under the guidance of J. W. Harvey at the Kitt–Peak Observatory (KPO). And finally, the third series of data was obtained at the Wilcox Solar Observatory of the Stanford University (WSO) and was made available to us by J. T. Hoeksema. These observations started in May 1976 (Carrington rotation 1641) and presently continue. If the photospheric magnetic field is known, then, using potential approximation and the source surface hypothesis, one can calculate the source surface field, i.e. the field at the origin of the heliosphere (Hoeksema & Sherrer 1986). In our analysis, we have used all three data series in spite of their nonuniformity. The data were reduced to a single scale by comparing the overlapping time intervals. As a result, the data on global magnetic fields and on three–dimensional structure of the heliosphere are now available for the past 35 years (more reliable for the past 29 years). We can also use the information on the Interplanetary Magnetic Field data (IMF data) based on the direct measurements nearly Earth for approximately the same time interval.

The behaviour of the correlation coefficient of B_{ss}/r^2 with B_x, $R_0(t)$, is illustrated in Fig. 3. One can readily see that during the first 10 years, correlation was rather low. Then, it increased gradually, and by the middle of the 80–ies it

had reached 60–70%. It is not quite clear, whether we deal with a real physical change of correlating values, or whether the effect is due to nonuniformity of our data series. Anyway, we can be sure that since 1976 the data are quite uniform, and therefore Fig. 5 positively displays a cyclic variation in the relation between the fields near the Earth and at the source surface.

Fig. 4 illustrates the transport time defined as a time shift of the main maximum of the cross–correlation function, $R_0(B_{ss}/r^2, B_x)$. We believe it to be the parameter that best characterizes variations of the mean mass velocity with the phase of the solar cycle. The shift is seen to be maximum in the middle of the 60–ies (minimum of the solar cycle). Then, it decreased gradually to reach its minimum value by the middle of the 80–ies. Only time will show, whether the present–day growth of the shift is a real tendency, and whether we do observe a certain cyclic variation. After 1976 the cyclic variation is practically absent.

And finally, Fig. 5 shows the relation between the field at the Earth orbit calculated from the scheme described above and the direct measurements. Here, two remarkable effects draw our attention. First, in the growth phase of all three cycles under consideration (20, 21, and 22), the measured fields are an order higher that the calculated ones. At other times, the difference does not exceed factor 2.5. Secondly, one can readily see that the data before and after 1976 are not alike. Before 1976, the calculated and the measured values agree amazingly well. After 1976, the measured values are at least twice as large as the calculated ones. It looks as if the MWO data used before 1976 were systematically different from the WSO data used after 1976.

References

Hoeksema, J.T., & Scherrer, P. H. 1986, Solar Magnetic Field 1976 through 1985, Report UAG–94, WDCA, Boulder

Lotova, N. A. 1988, Solar Phys., 117, 399

Lotova, N. A., Blums, D. F., & Vladimirsky, K. V. 1985, A&A, 150, No. 2, 266

Obridko, V. N. & Shelting, D. B. 1987, Geomagnetism and Aeronom., 27, No. 2, 97

Obridko, V. N. & Shelting, D. B. 1988, Kinematics and Physics of Celestial Bodies, 4, No. 4, 29

Parker, E. N. 1958, ApJ, 128, 664

Priest, E. R. 1985, Solar Magnetohydrodynamics, Mir, Moscow

Veselovsky, I. S. 1989, Solar Magnetic Fields and Corona, Novosibirsk, Nauka, 161

Wang, Y. M., & Sheely, N. R. 1990, ApJ, 355, 726

Wang, Y. M., & Sheely, N. R. 1991, ApJ, 372, L45

Wang, Y. M., Sheely, N. R., & Nash, A. G. 1990, Nature, 347, No. 6292, 439